

## DESIGN AND TESTING OF A FULLERENE RF ION ENGINE

John R. Anderson\*, Dennis Fitzgerald\*,  
Stephanie Leifer\* and Juergen Mueller\*

Jet Propulsion Laboratory  
California Institute of Technology  
Pasadena, California

Abstract

Because of the large mass, low first ionization potential and large electron impact ionization cross-section, it has been suggested that use of Buckminsterfullerene (C<sub>60</sub>) as a propellant might result in significant increases in ion engine efficiency over that obtained with xenon at low specific impulse. Because fullerenes decompose at an appreciable rate when exposed to temperatures greater than 800° C, it is desirable to eliminate hot cathode surfaces so testing of fullerene propellant was conducted using a RF ion engine. The RF engine was successfully operated using xenon; however, it was found that when the number flow rate of fullerene-to-xenon exceeded 1-to-16 the discharge would quench. The reason for this is that fullerenes have a large cross-section for electron attachment and a comparison of rate factors for positive and negative fullerene ion production shows that an electron temperature greater than 10 eV is needed to sustain a fullerene discharge. Time-averaged Langmuir probe data show that electron energies greater than this are obtained in the RF engine when it is operated on xenon. However, when fullerenes are added to the discharge high energy electrons become depleted and the discharge quenches when enough fullerene is added. Thus, conventional RF thrusters are unsuitable for operation on fullerenes.

Introduction

Because of the large mass, low first ionization potential and large electron impact ionization cross-section, it has been suggested that use of Buckminsterfullerene (C<sub>60</sub>) as a propellant might result in significant increases in ion engine efficiency over that obtained with xenon for missions requiring specific impulse in the 1,000 to 3,000 s range [1,2]. Since 1991, three groups [3-5] have reported on the development of ion thrusters which utilize fullerenes as a propellant. Anderson and Fitzgerald [3], and Hruby et al. [4] both successfully sustained fullerene plasma arc discharges using thoriated tungsten filament cathode ion sources. Anderson and Fitzgerald were able to extract beam currents between 2 and 3 mA from their device with a net accelerating voltage of 1.9 kV and a minimum discharge voltage of 22 V. They confirmed the presence of fullerene ions by mass spectral analysis of the extracted ion beam. Hruby et al. detected fullerene material deposited on optical surfaces using Fourier transform infrared (FTIR) spectroscopy. Both of these groups reported substantial erosion of the filament

cathodes used in their devices that ultimately resulted in cathode failure. The presence of a significant quantity of toluene-insoluble carbonaceous material was observed in the effusion cell by both groups after heating.

Hruby et al. carried out tests of fullerene material compatibility with stainless steel, molybdenum, alumina, boron nitride, aluminum nitride, and quartz. They reported that no reaction of the fullerenes occurred with any of these materials, but chose quartz for their discharge chamber with molybdenum and stainless steel grids. Anderson and Fitzgerald used both graphite and stainless steel sources and stainless steel grids. In both sources, notable degradation of the propellant molecules at high temperature was confirmed by FTIR spectroscopic analysis of the powder remaining in the effusive cell and on the walls of the discharge chamber. However, mass spectral analysis of the ion beam did not indicate the presence of C<sub>2</sub> fragments which would be expected from collisionally dissociate fullerenes [6].

Horak and Gibson [7] operated a commercially available Kaufman ion source with fullerenes for ion assisted deposition applications. They were able to sustain a discharge for 30 minutes while extracting a

---

\* Member of Technical Staff, Advanced Propulsion Group, Member AIAA

50-100  $\mu\text{A}/\text{cm}^2$  beam of fullerene ions. They reported that approximately 10% of the initial mass of  $\text{C}_{60}$  was recovered from the discharge chamber as a mixture of graphitic carbon and fullerene.

Takegahara and Nakayama [5] have reported an unsuccessful attempt to establish an RF-generated plasma using fullerenes. They found that their quartz discharge chamber wall temperature was too low, resulting in condensation of the fullerene propellant. Takegahara and Nakayama obtained FTIR absorption spectra of their  $\text{C}_{60}$  powder both before evaporation and after condensation. If normalized, their spectra indicate a loss of material similar to that observed by Hruby et al, and Anderson and Fitzgerald.

The observed degradation of fullerenes in these reports is a concern because the carbon residue could clog hollow cathodes and propellant feed lines. Flakes of residue could also short out the optics system grids [8]. In addition, decreased thruster efficiency due to extraction of an ion beam with a distribution of charge-to-mass ratio would result from extraction of ionized fullerene fragments. Since fullerenes became available in macroscopic quantities in 1991 [9], there have been several experimental studies of the thermal stability of  $\text{C}_{60}$  [10-12]. Frum et al, [13] observed thermal degradation of  $\text{C}_{60}$  heated to 1223 K while studying its infrared emission spectrum, while Sundar et al. [12] observed that solid  $\text{C}_{60}$  decomposes into amorphous carbon upon heat treatment beyond 993 K for 24 hours. Leifer et al. investigated solid state fullerene decomposition kinetics [14]. Fullerene degradation is attributed to solid-state unimolecular decay with an activation energy of 266 kJ/mol over the temperature range from 1073 to 1173 K. Thus in order to avoid significant propellant degradation, thruster operating temperatures must be maintained below approximately 1073 K.

### Experimental Apparatus

To avoid the presence of high temperature hollow cathode which typically operate at temperatures in excess of 1300 K, an RF discharge chamber similar to that of Takegahara and Nakayama [5] was constructed. An Eni Power Systems 13.56 MHz RF power generator (model 600A) and impedance matching circuit to reduce reflective RF losses from the engine were used. A schematic diagram and a photograph of the RF thruster assembly arc shown in Figs. 1 and 2, respectively.

The RF thruster, shown in Fig. 1, has a two-grid optics system and is mounted inside a 90 cm diameter by 150 cm long vacuum chamber capable of maintaining a no load pressure in the  $10^{-4}$  Pa (10<sup>-6</sup> Torr) range. The molybdenum grids are spaced 1.3 mm apart and have 331 matching 2.4 mm diameter holes with center-to-center spacing of 3.0 mm for an open area fraction of 0.29. The discharge chamber is enclosed

at the downstream end by the optics system, along the diameter by a 70 mm diameter, 70 mm long quartz vessel and at the upstream end by a quartz crucible. Wrapped around the quartz vessel is a 7 turn RF coil, made from 6.3 mm diameter copper tubing, which induces an alternating azimuthal electric field. To avoid fullerene condensation a heater wire, placed inside the RF coil tubing, is used to control the discharge chamber wall temperature.

The accelerator grid bias supply (100 mA D. C., up to 2.0 kV) is used to bias the accelerator grid negative with respect to ground. The screen grid, which provides the discharge chamber reference potential, is biased positive with respect to ground by the screen grid bias supply (100 mA D.C., up to 2.0 kV). The matching circuit located adjacent to the RF engine is used to match the load impedance to the 50  $\Omega$ , RG-213 coaxial transmission line. RF power is supplied by an Eni Power Systems 13.56 MHz RF power generator (model 600A).

The quartz crucible located at the upstream end of the discharge chamber is used to store fullerenes. when heated the fullerenes sublime and effuse into the discharge chamber. A small fraction of the fullerene mass flow in directed toward a water cooled Inficon model XTM/2 quartz crystal micro-balance (QCM). Real-time measurements of the rate at which fullerenes condense on the QCM can be correlated to the actual mass flow of fullerenes into the discharge chamber through a calibration constant.

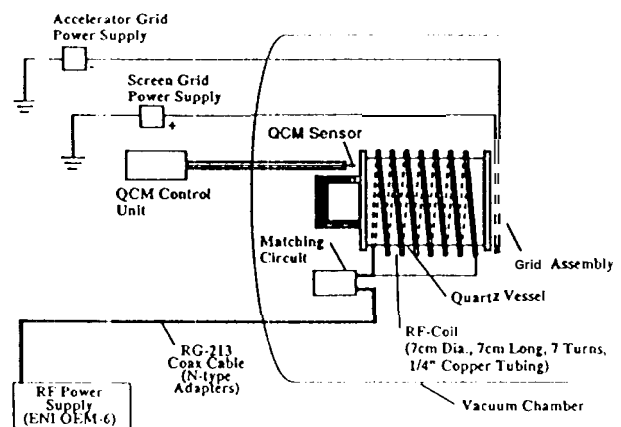


Fig. 1 Schematic diagram of fullerene RF thruster

A photograph of RF ion thruster mounted in the vacuum facility is shown in Fig. 2. The thruster coil is obscured by the presents of a stainless steel ground screen. A tungsten filament, used to start the RF discharge, can be seen in front of the accelerator grid. The discharge is initiated by heating the filament to thermionic emission temperatures and biasing both the screen and accelerator grids positive to draw

electrons into the discharge chamber while RF power is being supplied. Once the discharge has been ignited, the accelerator grid is biased negative to extract ions and stop electrons from backstreaming into the discharge chamber. At this point the filament can be left on to provide beam neutralizing electrons or it can be turned off and beam neutralizing electron can be provide from the vacuum tank walls.

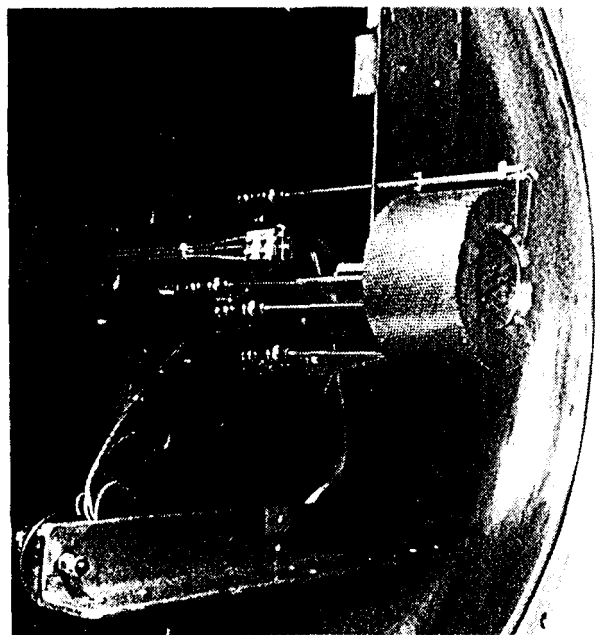


Fig. 2 Picture of RF Thruster

The quartz crucible used to store and evaporate fullerenes is shown in Fig. 3. The crucible has a 6 mm diameter tube fused to a coaxial 25 mm diameter tube in which fullerene powder is placed. The center tube is used to introduce test gases, such as xenon, into the discharge chamber. The flanged-crrd of the crucible attaches to the upstream end of the discharge chamber. A dam blocks the bottom half of the crucible to prevent fullerene spillage. This photograph was obtained after a preliminary test where the flanged-end of the crucible was not heated. The material at the flanged-end of the crucible is condensed fullerene while the material behind the quartz dam, which was heated, is amorphous and graphitic carbon residue. The small tube located slightly upstream of the dam is used to direct flow to the QCM sensor located approximately 70 mm away from the crucible.

Crucible temperature was monitored using a thermocouple mounted near the dam on the outside wall between the quartz and a heater which surrounds the crucible. Initial calibrations of crucible temperature were conducted with thermocouples attached to the inside walls as well as at the monitoring location. The temperature on the inside of the crucible was

approximately 40 to 50 K lower than the temperature measured at the monitoring location.

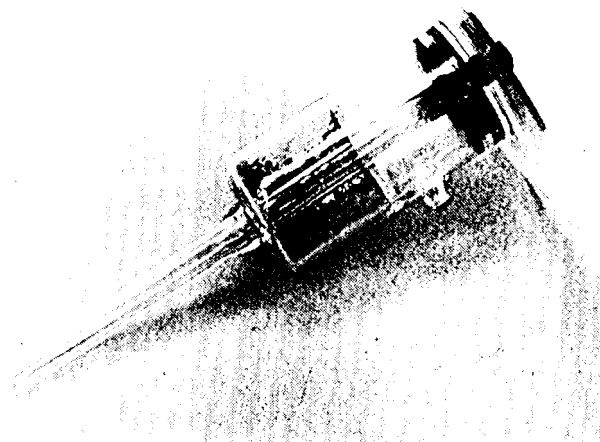


Fig. 3 Quartz Crucible

In addition to calibrating the crucible temperatures, discharge chamber wall temperature was calibrated as a function of heater power. To avoid RF interference with the thermocouples, the discharge chamber temperature was not monitored during experiments. Although the discharge chamber wall temperature was not monitored during testing, a reasonable estimate of the temperature could be obtained from the power being supplied to the chamber. The objective during most experiments was to keep the discharge chamber temperatures between 873 and 1073 K. This required providing between 250 and 450 W of heater power. The crucible and the discharge chamber arc not isolated thermally; as a result, the power input to both heaters influences the temperature of the whole system. Typically, the temperature varied by up to 100 K from hottest to coldest point in the discharge chamber-crucible system. The optics system was not heated directly and the screen grid was typically about 200 K colder than the hottest spot in the system.

The thermal calibrations were done with out RF power applied to the system; however, the RF power will influence the system temperature. It is noted that a large fraction of the RF power also goes into heating the chamber either from plasma diffusion to the walls, radiation to the walls or eddy current heating of the grids. Therefore, the power level to maintain the discharge chamber temperature is essentially the sum of the resistance heater power and the RF power.

The QCM is water cooled and the temperature of the QCM holder was found to be below 3(X) K during all experiments which is cold enough to keep fullerenes from sublimating from the QCM. Because

the geometry of the experimental apparatus does not change during a particular experiment, it is assumed that the fraction of the flow impinging on the QCM remains constant as the flow rate and RF thruster temperature vary. The system is taken apart between runs to resupply fullerenes to the crucible resulting in slight variations of alignment between the crucible and QCM from run to run; therefore, calibration constants are obtained for each run,

The calibration constant for total flow rate was determined by weighing the fullerene-filled crucible before and after heating to find the total mass of evaporated material. This quantity was then divided by the total accumulated mass on the qcm crystal to obtain the calibration constant C where

$$C = \frac{\Delta M}{\int_T \dot{m}_{qcm} dt} \quad (\text{Eq. 1})$$

where  $\Delta M$  is the total mass sublimated from the crucible,  $\dot{m}_{qcm}$  is the mass flow condensing on the qcm and the integration is over the time T during which fullerenes were flowing to the qcm. The actual mass flow rate to the discharge chamber  $\dot{m}$  is

$$\dot{m} = (C-1) \dot{m}_{qcm} \quad (\text{Eq. 2})$$

For typical experiments C is on the order of 8,000.

### Initial Experiments with RF Engine

To verify that a discharge could be sustained and to obtain data on the thruster operating characteristics, the RF engine was first operated using xenon as the source gas. Shown in Fig. 4 is the extracted beam current as a function of RF power for total and net accelerating voltages of 2.5 and 1.5 kV, respectively. The two curves shown correspond to flow rates of 0.25 and 0.15 mg/s. The maximum xenon ion current (space-charge limited) which could be extracted through the optics system was 42 mA. The minimum beam-ion energy cost for the higher flow rate case was found to be approximately 2,600 CV per beam ion. The efficiency of this engine could be improved significantly if the existing grids were replaced with a high open-area fraction, high perveance optics system. However, since the goal of these tests was to determine if a fullerene discharge could be sustained, the cost of a better optics system was not felt to be justified. In addition, higher efficiency could be achieved for a smaller surface-to-volume ratio discharge chamber which reduces diffusion

losses. The small size of the discharge chamber was chosen because limited quantities of fullerene (a few gm) were readily available. With the small thruster size tests lasting on the order of 1 hr could be run with less than a gm of fullerene.

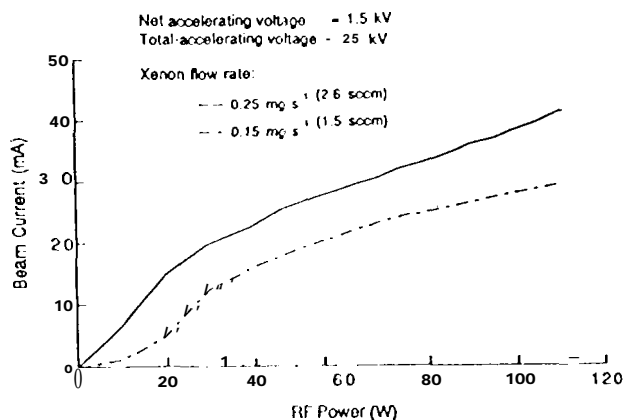


Fig. 4 Extracted Beam Current vs. RF Power

Based on the operating characteristics of the RF thruster operating on xenon, estimates of expected operating characteristics with C<sub>60</sub> were made. The space-charge limited C<sub>60</sub> current for the optics system operating with net and total accelerating voltages of 1.5 and 2.5 kV, respectively, is about 18 mA. The cross-section for positive ion formation of C<sub>60</sub> is an order of magnitude larger than that for xenon [15, 16]; therefore, the number density of fullerene required to sustain a discharge comparable to that obtained with xenon is an order of magnitude lower. Because C<sub>60</sub> has a mass of 720 a.m.u. compared to 131 a.m.u. for xenon, the fullerene mass flow rates expected to produce comparable plasma densities to those obtained at the xenon flow shown in Fig. 4 are .013 and .008 mg/s.

Shown in Fig. 5, is a plot of fullerene mass flow rate into the discharge chamber as a function of time. As seen in Fig. 5, fullerene flow rates greater than .20 mg/s (1.1 mg/s of xenon would be required to provide the same number flow rate) were provided to the engine for ~7.5 minutes. Between 300 and 600 W of power was provided to the thruster during this run so the wall temperature should have been over high enough to keep C<sub>60</sub> from condensing. Repeated attempts were made throughout this test to ignite a fullerene discharge with from 10 to 300 W of RF power being supplied to the engine; however, a sustained discharge was not achieved. Additional testing conducted by starting a xenon discharge and then adding fullerenes to the xenon flow was performed. During this testing it was found that when the ratio of fullerene to xenon neutrals exceeded 1:16 (data from 8-28-94), the plasma extinguished. This result led to suspicion that C<sub>60</sub>

anion formation was responsible for quenching the plasma.

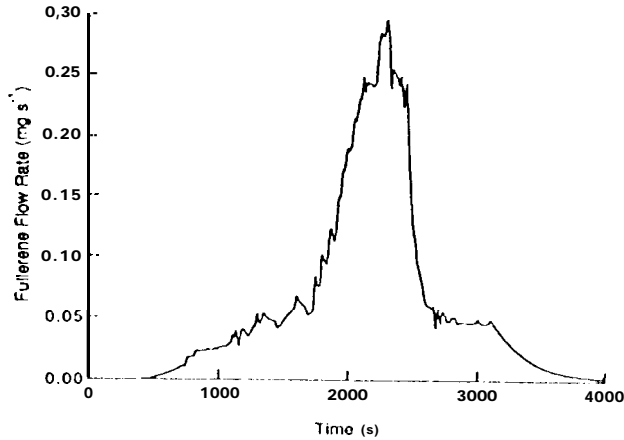


Fig. 5 Fullerene Mass Flow Rate vs. Time

### Rate Factor Estimates

One difference between C<sub>60</sub> and noble gas propellants is that C<sub>60</sub> has a large cross-section for negative ion formation, even at electron energies as high as 14 eV [17-19]. Due to the large cross-section for anion formation, electron attachment can dominate over positive ion formation for a low energy electron group. If this occurs, the C<sub>60</sub> behaves as an electron scavenger and the discharge can be quenched. Because a discharge in the RF thruster must be self sustaining, the positive ion formation rate must exceed the anion formation rate. The electron energy distribution in a typical RF discharge has a Maxwellian group and a higher energy electron group [20]. It is recognized that the high energy electrons contribute to cation formation and not to negative ion production. Therefore, computation of negative and positive ion production rates based on a thermal electron energy distribution results in a conservative estimate of the electron temperature required to sustain C<sub>60</sub> RF discharge.

To estimate the ion production rates in a plasma, peak intensities for positive and negative ion production shown in the literature [15,19] were used to obtain rate factors for ion production  $\langle\sigma v\rangle$ . It was assumed that the electrons used to acquire these data have a monoenergetic distribution. The rate factor for ion production resulting from collisions with an electron group in the plasma is

$$\langle\sigma v\rangle = \frac{\int_0^{\infty} \sigma v \, dn}{\int_0^{\infty} dn} \quad (\text{Eq. 3})$$

The term in the denominator is a constant and is equal to the total number density of electrons.

The differential form of Maxwell's law for the distribution of velocities is given by

$$dn = \frac{2\pi n \sqrt{E}}{(\pi k_B T)^{3/2}} C \exp\left(-\frac{E}{k_B T}\right) dE \quad (\text{Eq. 4})$$

Substituting Eq. 4 into Eq. 3 yields,

$$\langle\sigma v\rangle = A \int_0^{\infty} \sigma E \exp\left(-\frac{E}{k_B T}\right) dE \quad (\text{Eq. 5})$$

where  $A = 2\pi n \sqrt{2/m} / (\pi k_B T)^{3/2} \int_0^{\infty} dn$ . By

substituting  $\sqrt{E}\langle\sigma\sqrt{E}\rangle$  for  $\sigma E$  in Eq. 5, rate factors were determined using cross section data for negative fullerene ion formation from Reference [19] and the cross-section for C<sub>60</sub><sup>+</sup> formation shown in Reference [21] normalized to the data of Sai Baba [15]. Rate factor curves for C<sub>60</sub> as a function of electron temperature are shown in Fig. 6. For comparison the

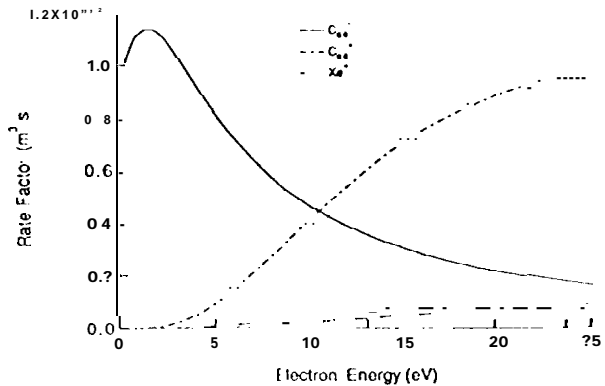


Fig. 6 Rate Factors vs. Electron Temperature

rate factor for xenon ion formation is shown. Cross-section data for xenon were obtained from Reference [16]. It is evident that negative fullerene ion production rates exceed those of positive ion production at electron energies below approximately 10 eV.

### Langmuir Probe Data

To obtain information on the electron energy distribution in the RF thruster, a Langmuir probe was installed in the discharge chamber. The probe consists of 0.25 mm diameter tungsten wire approximately

3 mm long which is exposed to the plasma. The wire leading up to the probe is jacketed by an alumina tube. The probe is located on the thruster axis, 27 mm from the screen grid. Typically, plasma densities are high enough during experiments that the probe erodes substantially. After 3.5 hrs of plasma exposure the diameter had decreased to 0.12 mm and the length had decreased to 2.4 mm.

Shown in Fig. 7 arc Langmuir probe traces obtained with the RF thruster operating with 200 W of RF power and a xenon flow rate of .21 mg/s. In this case, the grids on the screen and accelerator grids were biased at vacuum tank ground, so the system was operated without beam extraction. Traces shown were obtained with 0, 0.007 and 0.011 mg/s fullerene flowing into the discharge chamber. Addition of increasing amounts of fullerene to the flow results in increasingly sharper rises in negative current as probe potential increases. The electron energy distribution function is proportional to the second derivative of probe current with respect to probe voltage [22]. Generally it is difficult to obtain second derivatives of experimental data without amplifying noise to the point where it dominates. Williams [23] used a Fourier series smoothing technique to compute second derivatives.

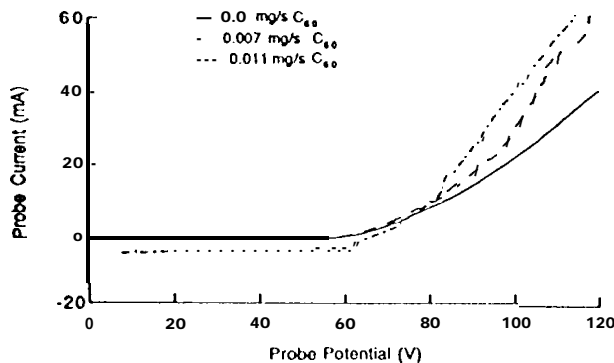


Fig. 7 Langmuir Probe Traces

The technique introduces smoothing errors. Additional errors associated with determining plasma potential from Langmuir probe as well as the rounding of the probe trace near plasma potential make obtaining accurate quantitative electron energy distribution functions difficult. Nevertheless the technique does give useful qualitative information on trends that occur as operating conditions are changed.

Shown in Fig. 8 arc the electron energy distribution functions estimated from the data shown in Fig. 7. These distribution functions were all normalized to unity. The distribution function with pure xenon is seen to have a large high energy group centered at about 60 eV and a low energy group. As fullerene is introduced to the discharge chamber, the distribution shifts toward a Maxwellian distribution and the magnitude and energy of the high energy group

decreases. When the fullerene flow rate was increased to 0.012 mg/s the plasma extinguished.

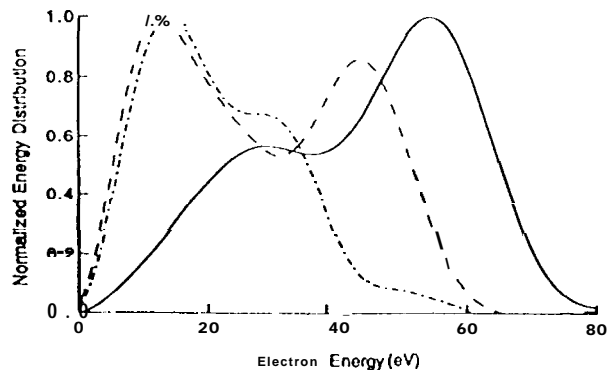


Fig. 8 Electron Energy Distribution Functions

The exact reason why the high energy electrons become depleted as fullerene is added to the discharge is not known. Fullerenes remove low energy electrons from the discharge when they form negative ions, so a depletion of low energy electron would be expected. Collisions, however, would tend to replenish the low energy electron group. In addition, it is noted that time averaged current are measured with the Langmuir probe. The electrons are being accelerated and decelerated during each RF cycle and the high energy electron group may have this high energy during a small fraction of the RF cycle. During a portion of the cycle they may be slowed to a low enough energy that they could combine with fullerenes. Such electrons would be lost and not re-accelerated, resulting in an apparent decrease in high energy electrons.

From the Langmuir probe data it appears that electron energies are high enough to sustain a fullerene discharge; yet, experimentally that is not the case. As previously discussed, the electron energy varies during each cycle and electrons are lost due to negative ion formation during the low energy portion of the cycle. It should be feasible to improve thruster efficiency by adding an electro-magnet to induce an axial magnetic field to reduce diffusion losses. In addition if a discharge could be sustained with a fullerene-to-xenon ratio greater than 1:1, it might be possible to increase electron energy enough to sustain a fullerene discharge by setting the gyro-frequency equal to the RF-frequency. Of course, as the ratio decreases it becomes increasingly more unlikely that this approach will work.

Some data showing the fraction of fullerene-to-xenon required to quench a xenon discharge as a function of RF power appears in Fig. 9. These data were obtained with the optics system grids biased at vacuum tank reference. The xenon flow rate was 0.21 mg/s and fullerene flow was increased until the discharge quenched. As seen here, the ratio of fullerene-to-xenon required to quench the discharge increases as RF power

increases. At 200 W the ratio of fullerene-to-xenon molecules required to quench the discharge is 1:145. The largest ratio which has been achieved with this RF thruster is 1:16 with the thruster operating with a xenon

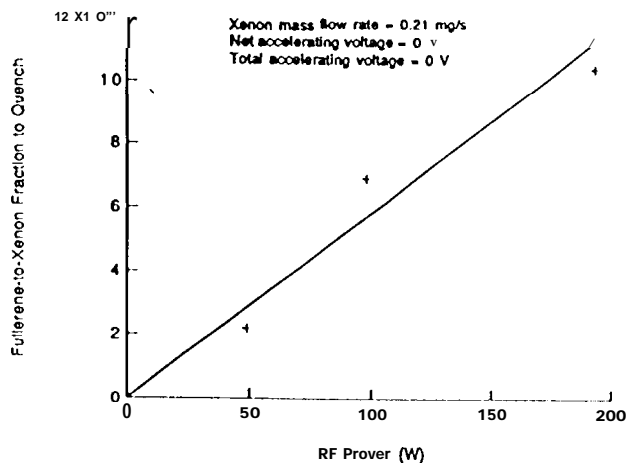


Fig. 9 Fullerene-to-xenon Ratio Required to Quench Discharge

flow rate of 0.3 mg/s and RF power of 350 W. The fact that such a small fraction of fullerene quenches the discharge means that it is unlikely that a fullerene discharge could be sustained with this particular RF thruster configuration.

### Conclusions

The feasibility of using fullerenes as a propellant in a conventional RF thruster was studied. It was determined that a self sustained RF discharge could not be achieved in such a thruster because fullerenes scavenge plasma electrons to form negative ions. In order to operate a thruster on fullerenes a method of supplying high energy electrons is needed. Sustained fullerene discharges have been achieved using filament cathodes to supply high energy electrons; however, thermal degradation of fullerenes has been observed in these discharges. Avoiding problems associated with thermal decomposition precludes use of cathodes operating at temperatures greater than 1073 K. Future work on fullerene thrusters should include studying the feasibility of constructing a field emission cathode capable of operating at low temperature and providing ampere level currents for thousands of hours. Another option would be to investigate the using of multipole RF antennas for sustaining the RF discharge. Such a system could be set up to operate in a manner similar to a 3-phase induction motor. By having a continuously rotating electric field it might be possible to keep the electron energy high enough to sustain an RF discharge.

### Acknowledgments

The research described in this paper was conducted at the Jet Propulsion Laboratory, California Institute of Technology, under contract with the National Aeronautics and Space Administration.

The authors thank A. G. Owens, W. R. Thogmartin and R. L. Toomath for their technical assistance.

### References

1. Leifer S., Rapp D., Saunders W., "Electrostatic Propulsion Using C<sub>60</sub> Molecules," AIAA Journal of Propulsion and Power, Vol. 8(6), 1993, p.1297
2. Torres E., Matossian J., Williams J., Martinez-Sanchez M. "predictions of the Performance of an Ion thruster Using Buckminsterfullerene as the Propellant," AIAA/SAE/ASME/ASEE 29th Joint Propulsion Conference AIAA 93-2494, Monterey, California, 1993.
3. Anderson J., Fitzgerald D., "Experimental Investigation of Fullerene Propellant for Ion Propulsion," IEPC-93-033, 1k.attic, Washington, Sept. 1993.
4. Hruby V., Martinez-Sanchez M., Bates S., Lorents D., "A High Thrust Density, C<sub>60</sub> Cluster Ion Thruster," 25th AIAA Plasmadynamics and Lasers Conference AIAA 94-2466, Colorado Springs, Colorado, June 1994.
5. Takegahara H., Nakayama Y., "C<sub>60</sub> Molecule as a Propellant for Electric Propulsion," 23rd International Electric Propulsion Conference IEPC-93-032, Seattle, Washington, Sept. 1993.
6. O'Brien S., Heath J., Cud R., Smalley R., "Photophysics of Buckminsterfullerene and Other Carbon Cluster Ions," Journal of Chemical Physics, Vol. 88, 1988, p. 220.
7. Horak P., Gibson U., "Broad Fullerene-Ion Beam Generation and Bombardment Effects," Applied Physics Letters, 65(8), 1994, p.968.
8. Brophy J., Polk J., Pless L., "Test-to-Failure of a Two-Grid, 30-cm-dia. Ion Accelerator System," IEPC-93-172, 23rd International Electric Propulsion Conference, Seattle, Washington, Sept. 1993.

9. Kratschmer W., Lamb L., Fostiropoulos K., Huffman D., "Solid C<sub>60</sub>-a New Form of Carbon," Nature, Vol. 347, 1990, p.354.
10. Von Gersum S., Kruse T., Roth P., "Spectral Emission During High Temperature Pyrolysis of Fullerene C<sub>60</sub> in Shock Waves," Berichte Bunsen-Gesellschaft für Physikalische Chemie, vol. 98(7), 1994, p. 979.
11. Kolodney E., Tsipinyuk B., Budrevich A., "The Thermal Stability and Fragmentation of C<sub>60</sub> Molecules up to 2000 K on the Millisecond Timescale," Journal of Chemical Physics, vol. 100(11), 1994, p. 8452.
12. Sundar C., Bharathi A., Harihan Y., Janaki J., Sankare Sastry V., Radhakrishnan T., "Thermal Decomposition of C<sub>60</sub>," Solid State Communications, Vol. 84(8), 1992, p. 823.
13. Frum C., Engleman R., Hedderich H., Bernath P., Lamb L., Huffman D., "The Infrared-Emission Spectrum of gas-Phase C<sub>60</sub> (Buckminsterfullerene)," Chemical Physics Letters, Vol.176(6),1991, p. 504.
14. Leifer S., Goodwin D., Anderson M., Anderson J., "Thermal Decomposition of a Fullerene Mix," Physical Review B, Vol. 51(15), 1995, p. 9973.
15. Sai Baba M., Narasimhan T., Balasubramanian R., Mathews C., "Appearance Potential and Electron Impact Ionization Cross-Section of C<sub>60</sub>," International Journal Of Mass Spectrometry and Ion Processes, Vol. 114, 1992, p. R1.
16. Rapp, D., and Englander-Golden, P., "Total Cross Sections for Ionization and Attachment in Gases by Electron Impact. 1. Positive Ionization," Journal of Chemical Physics, Vol. 34, No. 5, 1965, pp. 1464-1479.
17. Lezius M., Scheier P., Foltin M., Dunser B., Rauth T., Akimov V., Kratschmer W., Mark T., "Interaction of Free Electrons with C<sub>60</sub>: Ionization and Attachment Reactions, " International Journal of Mass Spectrometry and Ion Processes, Vol. 129, 1993, p. 49.
18. Lezius M., Scheier P., Mark T., "Free Electron Attachment to C<sub>60</sub> and C<sub>70</sub>," Chemical Physics Letters, Vol. 203(2,3), 1993, p. 232.
19. Jaffke T., Illenberger E., Lezius M., Matejcik S., Smith D., Mark T., "Formation of C<sub>60</sub><sup>-</sup> and C<sub>70</sub><sup>-</sup> by Free Electron Capture: Activation Energy and Effect of the Internal Energy on Lifetime," Chemical Physics Letters, vol. 226, 1994, p. 213.
20. Okuno Y., Ohtsu Y., Komatsu C., Fujita H., "Measurements of electron energy distribution function in an asymmetric radio-frequency discharge plasma," Journal Of Applied Physics, Vol. 73(4), 1993, p. 1612.
21. Leifer S., "Characterization of Fullerene for Electrostatic Propulsion Applications," Ph.D. Thesis, California Institute of Technology, Pasadena, California, May 1995.
22. Swift J., Schwar M., Electrical Probes for Plasma Diagnostics, Elsevier Publishing Company, Inc., New York, 1977, p. 80.
23. Williams J., "Plasma Contactor Research- 1990," NASA CR-187097, 1991, p. 57.